Dopability, Intrinsic Conductivity, and Nonstoichiometry of Transparent Conducting Oxides

Stephan Lany and Alex Zunger
National Renewable Energy Laboratory, Golden, Colorado 80401, USA
(Received 7 September 2006; published 23 January 2007)

Existing defect models for In_2O_3 and ZnO are inconclusive about the origin of conductivity, nonstoichiometry, and coloration. We apply systematic corrections to first-principles calculated formation energies ΔH, and validate our theoretical defect model against measured defect and carrier densities. We find that (i) intrinsic acceptors (''electron killers'') have a high ΔH explaining high n-dopability, (ii) intrinsic donors (''electron producers'') have either a high ΔH or deep levels, and do not cause equilibrium-stable conductivity, (iii) the O vacancy V_O has a low ΔH leading to O deficiency, and (iv) V_O has a metastable shallow state, explaining the paradoxical coexistence of coloration and conductivity.

DOI: 10.1103/PhysRevLett.98.045501 PACS numbers: 61.72.Bb, 61.50.Nw, 65.40.Gr, 71.15.Nc

Most metal oxides are insulators, even when band theory predicts them to be metallic (i.e., ''Mott Insulators'' [1]). An interesting opposite case is when oxides are electrically conductive, even though band theory predicts them to have wide band gaps. This behavior defines the materials class of ''transparent conductive oxides'' (TCO's) [2] such as ZnO, In_2O_3, and SnO_2, which have large band gaps in the ultraviolet, yet the Fermi level is in the conduction band due to free-carrier producing centers. These materials exhibit a remarkable phenomenology: (i) Doping by extrinsic electron producers (e.g., Sn donors in In_2O_3 and Al donors in ZnO) leads to enormous electron densities approaching 10^{21} cm^{-3}. Thus, in contrast to most other large gap materials, ''electron-killers'' (i.e., intrinsic acceptor-defects such as the cation vacancy) do not form spontaneously even at extremely high Fermi levels [3] well above the conduction band minimum (CBM). (ii) In contrast to common oxides like MgO, even the pure (undoped) In_2O_3 and ZnO show considerable free-carrier densities up to the 10^{17}–10^{19} cm^{-3} range [4,5]. The source of this conductivity remains, however, a mystery: While unintentional H donor impurities were implicated [6], it is now clear that the conductivity exists even when H has been annealed out or is absent [5,7]. (iii) In_2O_3, ZnO, and SnO_2 show a pronounced nonstoichiometry, with an O deficiency up to 1%, even under equilibrium growth conditions, at high-temperature [4,8]. (iv) After annealing (in reducing, metal-rich conditions), In_2O_3 and ZnO develop an apparently paradoxical coexistence of coloration, which is indicative of deep centers (F^+ centers [9]), and conductivity, which is indicative of shallow centers [4,5].

To date, no defect model exists that would account for the above phenomenology in TCO's. Early models [4,8] had difficulties to estimate the formation energy of defects and remained speculative as to the source of intrinsic electron-producers. In recent years, first-principles calculations in In_2O_3 [10–12], ZnO [7,13–18], or SnO_2 [19] helped to clarify many of the factors involved in TCO behavior. However, the lack of systematic corrections for deficiencies in the local density or generalized gradient approximations (LDA or GGA) to density functional theory (DFT), as well as for spurious energy contributions due to the finite-supercell formalism, lead to a large spread in the predictions for ZnO. For example, published results for the formation energy ΔH of the neutral zinc vacancy V_{Zn}^0 under Zn-poor conditions ranges from 1.5 [13] to 7.5 eV [14], while ΔH of the neutral oxygen vacancy V_O^0 under O-poor conditions ranges from (unphysically negative) −0.8 [15] to 3.9 eV [17].

In the present Letter, we develop a predictive defect model for In_2O_3 and ZnO from first-principles calculations, applying systematic corrections to LDA/GGA and supercell errors. In order to validate our theoretical results against available experimental data, we compute experimentally accessible quantities, i.e., defect and carrier densities as shown in Figs. 1 and 2 (whereas the commonly computed defect formation energies are rarely measured). We find the following: (i) ''electron killers,'' such as the O interstitial O_i in In_2O_3 and the V_{Zn} in ZnO, are remarkably unstable in In_2O_3 and ZnO, so high concentrations ($\sim 10^{21}$ cm^{-3}) of electron-producing Sn or Al donors remain uncompensated, in contrast to the case in main group oxides MgO and CaO [20]. (ii) Intrinsic electron producers, i.e., V_O and the cation interstitials In_i/Zn_i, do not lead to more than 10^{14} cm^{-3} free electrons at room temperature in equilibrium, and, thus, fail to explain the observed electron densities of $\sim 10^{18}$ cm^{-3}. (iii) The nonstoichiometry up to 1% is due to abundant O vacancies, and not due to cation interstitials. (iv) The paradoxical coexistence of coloration and conductivity can be explained by a metastable conductive state of V_O in both materials. While the O vacancy causes optical F-center absorption similar as in MgO, the V_O defect state becomes—unlike in MgO—resonant inside the conduction band after photoexcitation, leading to persistent photoconductivity (PPC), which may account for the observed free-carrier densities in pure In_2O_3 and ZnO.

Methods.—We use the pseudopotential-momentum-space-formalism [21], with the GGA exchange correlation of Ref. [22], as implemented in the VASP code [23]. Defects are calculated in 72-atom supercells of wurtzite ZnO, and 80-atom supercells of bixbyite In_2O_3, at their respective

 © 2007 The American Physical Society

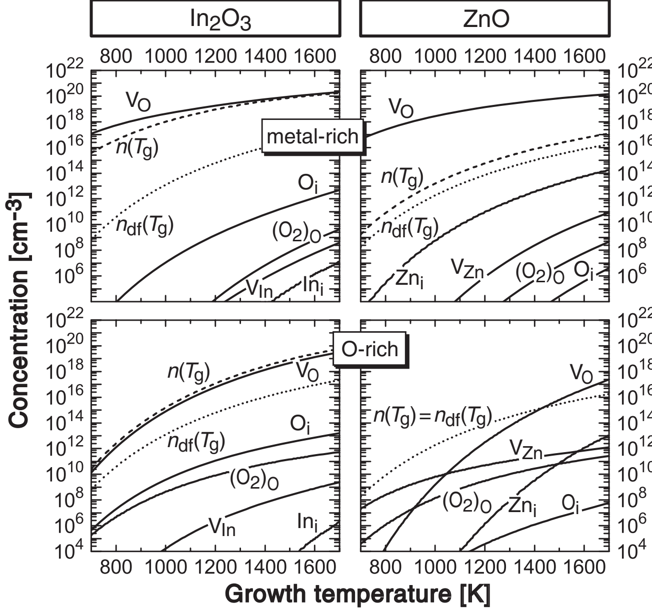

FIG. 1. Simulation of equilibrium grown pure In_2O_3 and ZnO: Calculated defect and electron (n) densities, as a function of growth temperature T_g. Top: Metal-rich conditions; $\Delta\mu_{In} = \Delta\mu_{Zn} = 0$. Bottom: O-rich conditions; $p(O_2) = 1$ atm. The electron density $n_{df}(T_g)$ due to thermal excitation across the band gap (without defects) is shown for comparison (dotted line).

GGA equilibrium lattice constant. The GGA band gaps are 0.94 eV in In_2O_3 and 0.73 eV in ZnO, much smaller than the experimental gaps 3.50 and 3.45 eV. We correct both GGA errors and finite-supercell errors according to the scheme described in Ref. [24] (see also below). We calculate the defect formation energy as

$$\Delta H_D(E_F, \mu) = [E_D - E_H] + qE_F + \sum \pm(\mu^0 + \Delta\mu),$$

where E_D and E_H are host + defect and host-only supercell energies, respectively, and q is the defect charge state. The chemical potentials $\Delta\mu_{In}$, $\Delta\mu_{Zn}$, $\Delta\mu_{Sn}$, $\Delta\mu_{Al}$, and $\Delta\mu_O$ for atoms added to $(-)$ or removed from $(+)$ the lattice are taken with respect to the GGA energy μ^0 of the elementary metals and the O_2 molecule. We apply the thermodynamic host stability condition, i.e., $2\Delta\mu_{In} + 3\Delta\mu_O = \Delta H_f(In_2O_3) = -8.12$ eV and $\Delta\mu_{Zn} + \Delta\mu_O = \Delta H_f(ZnO) = -2.93$ eV, where ΔH_f is the calculated oxide formation enthalpy. For $\Delta\mu_{Sn}$ and $\Delta\mu_{Al}$, we further consider the bounds imposed by formation of SnO_2 and Al_2O_3. The dependence of $\Delta\mu_O$ on the temperature and oxygen partial pressure $p(O_2)$ is calculated according to Ref. [20]. We also take into account the temperature dependence [4,25] of the band gap E_g, by which the energy E_C of the CBM is lowered. Having computed the corrected ΔH's, we perform thermodynamic simulations to obtain the defect and carrier densities, as well as the equilibrium Fermi energy E_F [26].

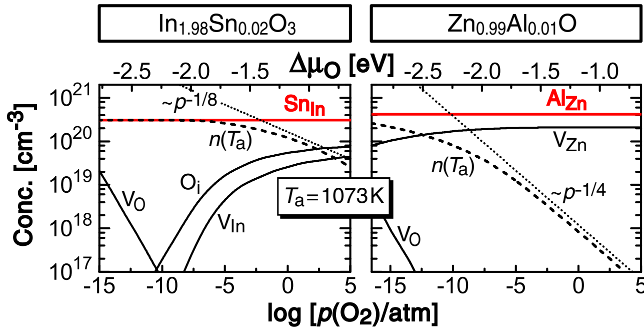

FIG. 2 (color online). Compensation of electron doped In_2O_3:Sn and ZnO:Al during annealing ($T_a = 1073$ K) in O_2 atmosphere. The thermodynamic simulations are constrained to a constant doping level of 1%, e.g., $[Sn]/([In] + [Sn]) = 0.01$. Shown are the calculated defect and carrier (n) densities, as a function of the oxygen partial pressure $p(O_2)$.

Intrinsic defects do not lead to shallow and abundant donors.—The calculated equilibrium concentrations of intrinsic defects and free carriers are shown in Fig. 1. While O vacancies form at concentrations up to the 10^{20} cm^{-3} range, cation interstitials are scarce, staying below 10^7 cm^{-3} in In_2O_3 and below 10^{14} cm^{-3} in ZnO. The calculated room-temperature electron density is very small, i.e., $n(RT) \leq 10^7$ cm^{-3} in In_2O_3 and $n(RT) \leq 10^{14}$ cm^{-3} in ZnO. The reason for the moderate carrier density is that V_O has a deep level which does not create free carriers, and that the formation energy of the cation interstitials is high (see Fig. 3). The low formation energy of the O vacancy originates from the formation of stable metal-metal bonds [16] between the In or Zn neighbors of V_O, which leads to strong atomic-relaxation and energy-lowering of the doubly occupied a_1^2 gap level. In contrast, the electrons introduced by In_i or Zn_i occupy a shallow level located at high energies close to the CBM, which leads to a large formation energy when E_F is high in the gap (Fig. 3). We conclude that intrinsic defects do not cause n-type conductivity under equilibrium conditions (see, however, below how the metastable state of V_O could lead to conductivity). The earlier suggestion of the Zn interstitial being the origin of conductivity in undoped ZnO [7,27] is in conflict with its large formation energy found here as well as in some of the previous calculations [14]. Indeed, Zn_i was experimentally observed only after its artificial generation by high-energy electron-irradiation [27,28]. Also, the suggestion [7] that a $(Zn_i - N_O)^+$ complex could cause n conductivity is, in fact, in contradiction with the theoretical results of the same work, which predicts pinning of the Fermi level at $E_V + 1$ eV [7], and, hence, insulating behavior [29]. Thus, a $(Zn_i - N_O)^+$ complex may form as a compensating donor in insulating ZnO, but it can not cause conductivity.

Even though the $(2+/0)$ donor level of V_O is deep at room temperature, we find in In_2O_3 an interesting deep-shallow transition due to the pronounced reduction of the band gap with temperature, bringing the donor level (cp. Fig. 3) closer to the CBM. This transition explains the observed drastic increase of *in situ* measured conduc-

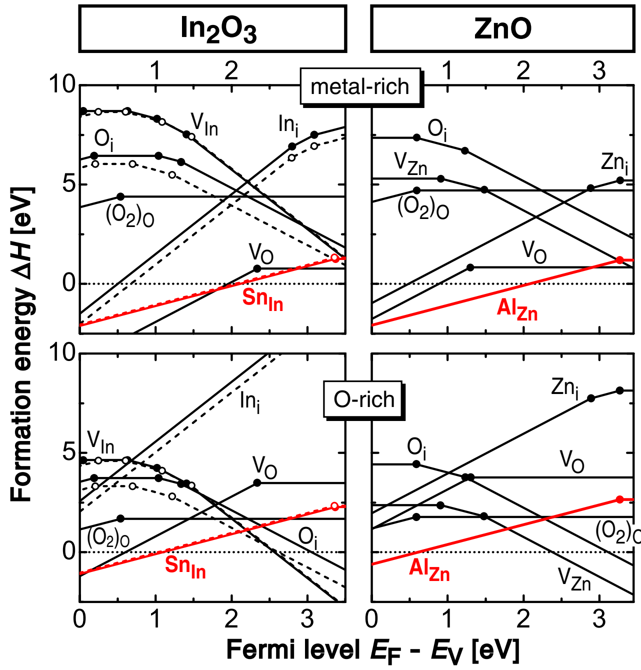

FIG. 3 (color online). Calculated defect formation energies as a function of E_F. The dots mark the transition energies between different charge states. In In_2O_3, the Wyckoff b (d) positions of the indium sites, and the a (c) positions of the interstitial sites are distinguished by solid (open) symbols and solid (dashed) lines. The metal- and oxygen-rich conditions are taken here as $\Delta\mu_{In} = \Delta\mu_{Zn} = 0$ and $\Delta\mu_O = 0$, respectively.

tivity above 1100 K [4], and leads to high-temperature electron concentrations comparable to the respective V_O concentrations (Fig. 1).

Extrinsic donors do lead to degenerate doping.—As shown in Fig. 3, Sn_{In} in In_2O_3 and Al_{Zn} in ZnO are shallow donors and have low ΔH even when E_F is near the CBM, and, therefore, can produce free carriers. We find that in In_2O_3, even the large donor concentration of 1% remains uncompensated for a wide range of growth conditions (O_2 partial pressures); i.e., the electron density equals the concentration of Sn donors (Fig. 2). In quantitative agreement with annealing experiments ($T_a = 1073$ K) [30], compensation occurs only at rather oxygen-rich conditions above $p(O_2) \gtrsim 10^{-6}$ atm, and leads to the observed [30] $p(O_2)^{-1/8}$ dependence of the electron density (Fig. 2). As seen in Fig. 3, the dominating electron killer O_i is ineffective under metal-rich conditions [low $p(O_2)$], having a formation energy still above 1 eV even when E_F is at the CBM. In ZnO, a donor concentration of 1% remains also uncompensated under extreme metal-rich conditions, as shown in Fig. 2. With increasing $p(O_2)$, however, the electron density falls short of the donor density, as a result of compensation by the V_{Zn} acceptor. The electron density follows a $p(O_2)^{-1/4}$ dependence above around $p(O_2) \geq 10^{-6}$ atm (Fig. 2), where strong compensation leads to nondegenerate electron densities and to a Fermi level inside the band gap ($E_F < E_C$). Note that vanishing formation energies of V_{Zn} when E_F approaches the CBM, as found in Refs. [13,15], are inconsistent with degenerate doping levels achievable in ZnO.

In nominally undoped ZnO with, e.g., $n = 10^{17}$ cm^{-3} (growth at $T_g = 1423$ K) [31], we obtain, in quantitative agreement with the positron annihilation experiments of Ref. [31], only small concentrations of compensating V_{Zn} defects, $c(V_{Zn}) = 2 \times 10^{15}$ cm^{-3} [at $p(O_2) = 1$ atm].

Large equilibrium oxygen deficiency.—In_2O_3 and ZnO are characterized by a large ($\lesssim 1\%$) O-deficient nonstoichiometry [4,8], which, historically, has been attributed to either the O vacancy, or the cation interstitial. Our calculations show that V_O, not the cation interstitial is the by far most abundant point defect in equilibrium grown In_2O_3 and ZnO (Fig. 1). In In_2O_3, the maximal calculated O vacancy concentration is 2×10^{20} cm^{-3} or 0.4% of the O lattice sites at $T = 1673$ K (Fig. 1, metal rich), agreeing well with the maximal O deficiency of 1% found in Ref. [4] from thermogravimetric analysis at this temperature. In ZnO, the calculated concentration of V_O is 4×10^{19} cm^{-3} (0.1%) at $T = 1373$ K (Fig. 1) under Zn-rich growth, where we chose conditions comparable with the coloration experiments in Ref. [5]. This maximal V_O concentration is consistent with the range of O deficiency of high-temperature equilibrium grown ZnO [8], and with $c(V_O) \approx 10^{17}$ cm^{-3} determined by positron annihilation spectroscopy in chemical vapor transport grown ZnO [32].

Excited O *vacancies can lead to (persistent) photoconductivity.*—The possibility that V_O could cause PPC in ZnO was surmised already in Ref. [14], and we recently developed a detailed model for PPC due to anion vacancies [16], finding that the ground state of V_O^0 has a deep, nonconductive a_1^2 level, but that the excited vacancy has a metastable conductive state. Following photoexcitation, the emptied a_1^0 level moves deep into the conduction band, giving up its two electrons to a shallow, conductive state near the CBM [16]. This behavior is found here also for In_2O_3, but not for the main group oxides, e.g., CaO [20], where the empty a_1^0 stays inside the gap. The back transition into the nonconducting ground state is impeded by an energy barrier, and ambient background illumination could be sufficient to constantly regenerate the conductive state due to the large optical cross section for F^+-center (V_O^+) excitation [9], explaining the residual conductivity of pure In_2O_3 and ZnO.

Coexistence of coloration and conductivity.—The simultaneous occurrence of coloration and conductivity after metal-rich growth, found both in In_2O_3 (gray) [4] and in ZnO (red) [5], creates an apparent paradox: On one hand, color centers are indicative of a deep level (i.e., the excitation $V_O^0 \rightarrow V_O^+ + e$ requires an energy in the visible range), but, the existence of conductivity is indicative of a shallow level. For the optical $V_O^0 \rightarrow V_O^+ + e$ and $V_O^+ \rightarrow V_O^{2+} + e$ excitations, we calculate 1.8 and 1.6 eV in In_2O_3 (present Letter), compared to 2.8 and 2.4 eV in ZnO [16].

These absorption energies, along with the large concentrations of V_O (Fig. 1), explain the gray and red coloration in reduced In_2O_3 and ZnO, as well as the recent observation of photoemission from a gap state [33] in In_2O_3. Room-temperature electron-densities in the 10^{17}–10^{19} cm^{-3} range [4,5,7] would require the simultaneous presence of large quantities of another, donorlike defect with a shallow level, such as hydrogen. However, doping levels up to the 10^{18} cm^{-3} range are also found in H-free ZnO [5,7]. Therefore, we propose that our model of V_O causing PPC would resolve the apparent paradox of coexisting coloration and conductivity.

Total-energy corrections.—(i) We correct the band gap by a downshift ΔE_V of the valence-band maximum, determined through GGA + U calculations, and by an upward shift ΔE_C of the CBM by the remaining band gap error [16,24] ($\Delta E_V = -0.28$ eV in In_2O_3 and $\Delta E_V = -0.69$ eV in ZnO). (ii) For shallow, hostlike levels, we apply corrections to ΔH according to the respective band-edge corrections ΔE_C and ΔE_V. For deep levels such as the oxygen and the cation vacancies [28], this correction is not applied. (iii) We eliminate band-filling effects due to the finite-supercell size [24], and account for the increased [34] donor formation energies due to the Moss-Burstein shift by considering the actual equilibrium electron density. (iv) The total energy of charged supercells is corrected by a potential alignment procedure [24]. (v) The effective (i.e., screened) Madelung energy of charged defects in the jellium background is corrected to $O(L^{-5})$.

Our correction scheme yields for the O vacancy in ZnO a deep $\varepsilon(2+/0)$ transition level at $E_C - 2.2$ eV, contrasting the much shallower level at $E_C - 1.0$ eV obtained by Janotti and van de Walle [17] who used an extrapolation scheme based on LDA + U. Recent, more advanced hybrid-DFT results [18], however, which yield the correct band gap energy of bulk ZnO, find the $\varepsilon(2+/0)$ level of V_O to be deep at $E_C - 3.0$ eV, and confirm our interpretation [16] of the optical magnetic resonance experiments by Vlasenko and Watkins [28]. We further note that the formation energy $\Delta H(V_O) \geq 3.9$ eV in n-type ZnO found by Janotti and van de Walle [17] implies V_O concentrations $c(V_O) \lesssim 10^8$ cm^{-3} far below the experimentally observed level of $c(V_O) \approx 10^{17}$ cm^{-3} [32]. Although self-interaction correction (SIC) of the LDA is expected to yield an accurate electronic structure, its limited implementation, i.e., the use of SIC-corrected atomic pseudopotentials in a non-SIC LDA supercell calculation [14], is not accurate enough to reproduce the deep state of the O vacancy in ZnO. Thus, the rather shallow energy $E_C - 1.0$ eV of the occupied a_1^2 level of V_O^0 in the pseudopotential-SIC scheme [14] is inconsistent with the experimental color-center absorption peaked at 3.0 eV [5], and with the hybrid-DFT results [18]. Our present correction scheme also successfully explained the optical absorption energies in the well-studied case of the F^+-center (sulfur vacancy) in ZnS [35].

In conclusion, we developed from first-principles calculations and thermodynamic simulations a comprehensive and validated defect model for the TCOs In_2O_3 and ZnO.

This Letter was funded by the U.S. Department of Energy, DOE-BES and DOE-EERE, under Contract No. DE-AC36-99GO10337.

[1] N. F. Mott, *Metal-Insulator Transitions* (Taylor & Francis, Ltd., London, 1974).
[2] Special issue on Transparent Conducting Oxides, edited by D. S. Ginley and C. Bright [MRS Bull. **25** (2000)].
[3] A. Zunger, Appl. Phys. Lett. **83**, 57 (2003).
[4] J. H. W. de Wit, J. Solid State Chem. **13**, 192 (1975); J. Solid State Chem. **20**, 143 (1977); J. H. W. de Wit, G. van Unen, and M. Lahey, J. Phys. Chem. Solids **38**, 819 (1977).
[5] L. E. Halliburton *et al.*, Appl. Phys. Lett. **87**, 172108 (2005).
[6] C. G. van de Walle, Phys. Rev. Lett. **85**, 1012 (2000).
[7] D. C. Look *et al.*, Phys. Rev. Lett. **95**, 225502 (2005).
[8] F. A. Kröger, *The Chemistry of Imperfect Crystals* (North-Holland, Amsterdam, 1974).
[9] J. M. Smith and W. E. Vehse, Phys. Lett. A **31**, 147 (1970).
[10] O. N. Mryasov and A. J. Freeman, Phys. Rev. B **64**, 233111 (2001).
[11] I. Tanaka *et al.*, J. Am. Ceram. Soc. **85**, 68 (2002).
[12] O. Warschkow *et al.*, J. Am. Ceram. Soc. **86**, 1700 (2003).
[13] A. F. Kohan *et al.*, Phys. Rev. B **61**, 15 019 (2000).
[14] S. B. Zhang, S. H. Wei, and A. Zunger, Phys. Rev. B **63**, 075205 (2001).
[15] E. C. Lee *et al.*, Phys. Rev. B **64**, 085120 (2001).
[16] S. Lany and A. Zunger, Phys. Rev. B **72**, 035215 (2005).
[17] A. Janotti and C. G. v.d. Walle, Nat. Mater. **6**, 44 (2007).
[18] C. H. Patterson, Phys. Rev. B **74**, 144432 (2006).
[19] C. Kilic and A. Zunger, Phys. Rev. Lett. **88**, 095501 (2002).
[20] J. Osorio-Guillen *et al.*, Phys. Rev. Lett. **96**, 107203 (2006).
[21] J. Ihm, A. Zunger, and M. L. Cohen, J. Phys. C **12**, 4409 (1979).
[22] J. P. Perdew, K. Burke, and M. Ernzerhof, Phys. Rev. Lett. **77**, 3865 (1996).
[23] G. Kresseand and J. Joubert Phys. Rev. B **59**, 1758 (1999).
[24] C. Persson *et al.*, Phys. Rev. B **72**, 035211 (2005).
[25] F. J. Manjon *et al.*, Solid State Commun. **128**, 35 (2003).
[26] S. Lany *et al.*, Appl. Phys. Lett. **86**, 042109 (2005).
[27] D. C. Look, J. W. Hemsky, and J. R. Sizelove, Phys. Rev. Lett. **82**, 2552 (1999).
[28] L. S. Vlasenko and G. D. Watkins, Phys. Rev. B **71**, 125210 (2005); Phys. Rev. B **72**, 035203 (2005).
[29] From our thermodynamic simulations we find that a Fermi level within 0.5 eV from the CBM is needed during growth or annealing to warrant a net n doping of 10^{17} cm^{-3}.
[30] G. B. Gonzales *et al.*, J. Appl. Phys. **96**, 3912 (2004).
[31] F. Tuomisto *et al.*, Phys. Rev. Lett. **91**, 205502 (2003).
[32] F. Tuomisto *et al.*, Phys. Status Solidi B **243**, 794 (2006).
[33] A. Klein, Appl. Phys. Lett. **77**, 2009 (2000).
[34] S. Lany, H. Wolf, and Th. Wichert, Phys. Rev. Lett. **92**, 225504 (2004).
[35] S. Lany and A. Zunger, Phys. Rev. Lett. **93**, 156404 (2004).